GMR
The Original

SUSTAINABLE DEVELOPMENT OF CuO NANOPARTICLES REINFORCED WITH STARCH/PVA ELECTROSPUN NANOSCAFFOLDS USING *Gracilaria corticata* EXTRACT FOR DIABETES MANAGEMENT

Aksitha Sakthiraj[1], Darshini Adhinathan[2], Abyramy Balasundaram[2], Alagendran Subbarayalu[3]*

[1]Saveetha Medical College & Hospital (SMCH), Saveetha Institute of Medical and Technical Sciences (SIMATS), Thandalam, Chennai, Tamil Nadu 602105, India. aksitha2004sakthiraj@gmail.com
[2]Department of Dermatology, Saveetha Medical College and Hospital, Saveetha Institute of Medical And Technical Sciences (SIMATS), Thandalam, Chennai-602105, Tamil Nadu, India. Email: darshiniadhinathan1998@gmail.com; b.abyramy@gmail.com.
[3]Clinical Neuroscience and Phytomedicine Laboratory, Department of Research, Saveetha College of Nursing (SCON), Saveetha Institute of Medical and Technical Sciences (SIMATS), Chennai 602105, Tamil Nadu, India. Email: proteinblg@gmail.com; alagendrans.scon@saveetha.com. ORCID: https://orcid.org/0009-0009-0749-7180.
*Correspondence: proteinblg@gmail.com; alagendrans.scon@saveetha.com (A.S.)

ABSTRACT
This study explores the green synthesis of copper oxide nanoparticles (CuO NPs) using *Gracilaria corticata* algal extract and their incorporation into starch/PVA nanoscaffolds for antidiabetic applications. UV-Vis spectroscopy confirmed CuO NP formation via a distinct surface plasmon resonance peak at 291 nm, while Fourier-Transform Infrared Spectroscopy (FTIR) analysis identified bioactive functional groups acting as reducing and stabilizing agents. X-ray diffraction (XRD) revealed a monoclinic crystalline structure, and scanning electron microscopy (SEM) demonstrated uniform NP dispersion within the nanofibrous scaffold (90–150 nm diameter) without aggregation. thermogravimetric analysis (TGA) indicated enhanced thermal stability due to CuO NP reinforcement, and dynamic light scattering (DLS) analysis showed moderate colloidal stability (Z-average: 68.6 nm; zeta potential: −14.11 mV). The antidiabetic potential was evaluated through α-amylase and α-glucosidase inhibition assays. The starch/PVA/CuO-NP nanoscaffolds exhibited superior enzyme inhibition (77.72–79.52% at 100 µg/mL) compared to standalone CuO NPs (67.72%) and crude extract (49.72%), highlighting synergistic effects. The concentration-dependent activity suggests promising applications in diabetes management by delaying carbohydrate digestion. This work underscores the efficacy of biogenic CuO NPs and their composite scaffolds, leveraging eco-friendly synthesis and enhanced bioactivity. Further *in vivo* studies and IC_{50} validation are recommended to advance therapeutic potential.

KEYWORDS: *Gracilaria corticata*, Green synthesis, CuO nanoparticles, starch/PVA/CuO-NPs nanoscaffolds, Antidiabetic activity.

1. INTRODUCTION

Diabetes mellitus is a chronic metabolic condition characterized by sustained hyperglycemia resulting from either insulin resistance or insufficient insulin production [1]. The disease poses a substantial public health challenge, with the International Diabetes Federation estimating that more than 537 million adults were affected globally in 2021, and this number is projected to exceed 640 million by 2030 [2]. The increasing incidence is largely attributed to sedentary lifestyles, unhealthy diets, and genetic predispositions [3]. Among the various forms of diabetes, type 2 diabetes mellitus (T2DM) is the most prevalent, accounting for over 90% of all cases [4]. Despite the availability of pharmacological agents such as sulfonylureas, biguanides, and alpha-glucosidase inhibitors, long-term use is often associated with adverse effects, including gastrointestinal distress, hypoglycemia, and organ toxicity [5]. Additionally, the economic burden of lifelong medication and the lack of accessible healthcare in under-resourced regions necessitate the exploration of alternative, sustainable therapeutic strategies [6].

Nanotechnology offers innovative solutions in biomedical research, particularly in drug delivery and therapeutic diagnostics [7]. Nanoparticles—materials with dimensions ranging from 1 to 100 nanometers—exhibit unique characteristics such as high surface area, quantum effects, and enhanced reactivity, which make them highly suitable for biological applications [8]. Among metal oxide nanoparticles, copper oxide nanoparticles (CuO NPs) have attracted significant attention due to their potent antibacterial, antifungal, anticancer, and antioxidative

activities [9]. Recent research suggests that CuO NPs can also modulate glucose metabolism by inhibiting digestive enzymes like α-amylase and α-glucosidase, which are responsible for breaking down complex carbohydrates into absorbable sugars [10]. By impeding these enzymes, CuO NPs can potentially reduce postprandial hyperglycemia, making them promising candidates for managing T2DM [11].

Traditional nanoparticle synthesis techniques often involve hazardous chemicals and energy-intensive conditions, raising concerns about environmental safety and biocompatibility [12]. In contrast, green synthesis approaches utilize biological organisms or natural extracts to reduce and stabilize nanoparticles in a more sustainable and eco-friendly manner [13]. Marine macroalgae, or seaweeds, are a particularly attractive choice for this process due to their abundance in oceans, renewable nature, and rich phytochemical composition [14].

Gracilaria corticata, a red marine macroalga, is known for its high content of sulfated polysaccharides, phenolics, proteins, and flavonoids [15]. These biomolecules can serve as natural reducing and capping agents during nanoparticle synthesis, enhancing the stability and functional performance of the resulting nanomaterials [16]. Extracts of *G. corticata* have previously been reported to exhibit diverse biological activities, including antioxidant, antimicrobial, and anti-inflammatory effects, making them highly suitable for biomedical applications [17]. The integration of such marine-derived bioactives in nanoparticle synthesis not only ensures a greener route but also imparts additional therapeutic potential to the nanoparticles [18].

Electrospinning is a versatile and cost-effective technique widely used for fabricating ultrafine fibers from polymer solutions [19]. The resultant nanofibrous scaffolds possess high porosity, tunable mechanical strength, and a large surface-area-to-volume ratio, which are advantageous for drug delivery, wound healing, and tissue regeneration [20]. In this context, biodegradable and biocompatible polymers such as starch and polyvinyl alcohol (PVA) have been extensively used [20]. Starch, a natural polysaccharide, offers excellent film-forming and hydrophilic properties, while PVA contributes mechanical stability and electrospinnability. When combined, these polymers produce composite nanofibers suitable for biomedical applications [21].

The functionalization of these polymeric scaffolds with green-synthesized CuO NPs using *G. corticata* extract can significantly enhance their therapeutic efficacy. Such incorporation enables the controlled and sustained release of bioactive agents, improves antioxidant and antibacterial properties, and provides enzymatic inhibitory action—thereby offering a multifaceted approach to managing diabetic complications [22].

The convergence of green nanotechnology and biomaterials engineering offers an innovative platform for antidiabetic interventions [23]. The biosynthesized CuO NPs using *G. corticata* extract present a unique blend of marine-derived bioactivity and nanomaterial functionality [24]. By incorporating these CuO NPs into starch/PVA electrospun scaffolds, it is possible to fabricate a biocompatible matrix with dual capabilities: (i) inhibiting carbohydrate-digesting enzymes and (ii) promoting wound healing and tissue regeneration, which is critical in diabetic patients [25].

Moreover, *G. corticata*-mediated synthesis eliminates the use of hazardous reagents, ensuring the final product is both eco-friendly and safe for therapeutic use [26]. Previous studies have highlighted the synergistic interaction between metal nanoparticles and polymer matrices in enhancing biological responses [27]. Therefore, this integrated approach holds promise for developing cost-effective, multifunctional, and sustainable materials for diabetes management and related complications [28].

The present study focuses on the synthesis, characterization, and biological evaluation of CuO NPs synthesized using *G. corticata* extract, and their subsequent incorporation into electrospun starch/PVA nanofibrous scaffolds for antidiabetic applications.

This research offers a multidisciplinary strategy that bridges marine biotechnology, green chemistry, and nanomedicine to develop a novel antidiabetic therapeutic material. By utilizing *G. corticata*, a renewable marine resource, for the synthesis of CuO NPs, the study supports sustainable practices while enhancing biomedical functionality. The resultant nanofibrous scaffolds are expected to exhibit strong inhibitory effects on carbohydrate-hydrolyzing enzymes, along with improved biocompatibility and potential wound-healing capabilities. Ultimately, this work could pave the way for the development of next-generation, eco-friendly biomaterials for managing diabetes and its complications.

2. MATERIALS AND METHODS

2.1 Chemicals and reagents

The brown macroalga *G. corticata* was collected from the coastal region of Rameswaram, Tamil Nadu, India, serving as a renewable natural resource for the green synthesis of CuO NPs. Copper (II) sulfate pentahydrate ($CuSO_4 \cdot 5H_2O$), obtained from Merck and of analytical grade, was used as the copper precursor. PVA with an

approximate molecular weight of 115,000 g/mol and starch were selected for fabricating biocompatible and biodegradable nanofibrous scaffolds. Electrospinning was performed on a HOLMARC HO-NFES-040 system. All other reagents and solvents used throughout the study were sourced from Sigma-Aldrich and Merck, ensuring analytical-grade quality to maintain experimental precision and reproducibility.

Characterization of synthesized nanoparticles and scaffolds utilized an array of analytical tools including UV–Visible spectrophotometry, Fourier-transform infrared (FTIR) spectroscopy, X-ray diffraction (XRD), scanning electron microscopy (SEM), dynamic light scattering (DLS), zeta potential analysis, and thermogravimetric analysis (TGA). Antidiabetic potential was evaluated by standardized *in vitro* assays.

2.2 Collection and processing of marine algae

Samples of the brown alga *G. corticata* were harvested from the intertidal zone along the Rameswaram coast. Immediately post-harvest, specimens were transported in refrigerated containers to preserve the integrity of bioactive compounds. The algal material was thoroughly rinsed with tap water to remove extraneous debris, sand, and epiphytes, followed by repeated washes with distilled water to eliminate residual salts and impurities. Approximately 100 grams of cleaned algae were chopped into smaller pieces and air-dried at ambient temperature for about two weeks. The dried biomass was then pulverized into a fine powder using a mechanical grinder and stored in airtight containers under cool, dry conditions until further use.

2.3 Ultrasonic-assisted extraction of bioactive constituents

Bioactive compounds were extracted from the powdered *G. corticata* using ultrasonic-assisted extraction (UAE) to improve yield through enhanced cellular disruption. Specifically, 2 grams of dried algal powder were suspended in 50 mL of Milli-Q water within a 100 mL borosilicate beaker. The suspension was subjected to ultrasonication at 60°C for 45 minutes using a LABQUEST ultrasonic cleaner (Borosil; Serial No. 941032329018). Following extraction, the mixture was filtered through sterile Whatman No. 1 filter paper to separate solids. The clear filtrate, containing soluble phytochemicals, was stored at 10°C under sterile conditions. A portion of this filtrate was freeze-dried using a laboratory lyophilizer to yield a stable powdered extract for use in CuO NPs synthesis [28].

2.4 Biosynthesis of CuO NPs

The green synthesis of CuO NPs was initiated by combining the algal extract with an aqueous copper salt solution. A 0.1 M $CuSO_4 \cdot 5H_2O$ solution (50 mL) was prepared, to which 10 mL of the algal extract (10 mg/mL) was added, maintaining a precursor-to-extract volume ratio of 5:1. The mixture was continuously stirred at 650 rpm and heated to 60°C for 2 hours on a magnetic stirrer equipped with a temperature-controlled hot plate. The transition of the solution color from deep blue to bluish-green visually indicated nanoparticle formation, corresponding to the reduction of Cu^{2+} ions by the algal phytochemicals. The resulting nanoparticles were washed thrice with double-distilled water to remove residual reactants and biomolecules. Finally, the CuO NPs were freeze-dried for 48 hours to obtain a fine, stable powder suitable for scaffold incorporation and biological testing [29].

2.5 Fabrication of starch/PVA nanofibrous scaffolds incorporating CuO NPs

Nanofibrous scaffolds were fabricated from a blend of starch and PVA loaded with biosynthesized CuO NPs. Initially, a 15% (w/w) solution of fully hydrolyzed PVA was prepared by dissolving the polymer in Milli-Q water under continuous stirring at 50°C until fully dissolved. Subsequently, 100 mg each of starch and CuO NPs were incorporated into the PVA solution, and the mixture was stirred further for 2.5 hours at 50°C to ensure homogenous dispersion.

The viscous composite solution was then loaded into a 10 mL syringe fitted with a stainless-steel needle (0.84 mm internal diameter). Electrospinning was conducted using the HOLMARC HO-NFES-040 device with optimized parameters: 11.5 kV applied voltage, a tip-to-collector distance of 12.3 cm, and a flow rate of 0.4 mL/h. The process was performed at room temperature over 6–8 hours. The resulting nanofibrous mats were carefully collected and stored in desiccators to maintain their structure and prevent moisture uptake [21, 30].

2.6 Physicochemical characterization

2.6.1 UV–Visible Spectroscopy

UV–Visible absorption spectra of the algal extract, biosynthesized CuO NPs, and CuO-loaded starch/PVA nanofibers were recorded using a VIS SPEC V-730 spectrophotometer. Scans were performed from 200 to 800 nm with deionized water as the blank reference. Characteristic absorption peaks between 270 and 300 nm were observed, consistent with surface plasmon resonance effects of CuO NPs [31].

2.6.2 FTIR Spectroscopy analysis

Functional group analysis and chemical interaction assessment were performed by FTIR using a PerkinElmer Spectrum Two spectrometer in ATR mode. Spectra were collected over the range of 4000–400 cm^{-1} with a resolution of 4 cm^{-1}, averaging 64 scans per sample. Key absorption bands corresponding to hydroxyl (O–H), carbonyl (C=O), amide, and metal-oxygen (Cu–O) groups were identified, confirming the integration of CuO NPs within the polymeric scaffold matrix [32, 33].

2.6.3 XRD analysis

The crystalline nature of CuO NPs and composite nanofibers was investigated using a Bruker D8 Advance diffractometer with CuKα radiation (λ = 1.5406 Å), operated at 40 kV and 40 mA. Diffraction patterns were collected over 2θ angles from 5° to 90° with a step size of 0.029649°. Characteristic sharp peaks corresponding to monoclinic CuO crystalline phase were detected, while peak shifts and broadening in composites suggested successful embedding of nanoparticles within the polymer network [34].

2.6.4 SEM analysis

Surface morphology and nanoparticle distribution within the nanofibrous scaffolds were examined using a JEOL JSM-IT800 NANO SEM. Samples were sputter-coated with a thin gold layer to enhance conductivity prior to imaging. Micrographs revealed uniform nanofiber formation with minimal bead defects and well-dispersed CuO NPs throughout the fibrous matrix [28].

2.6.5 TGA

Thermal stability tests were conducted using a PerkinElmer TGA 8000 instrument. Approximately 5 mg of each sample was heated from room temperature to 550°C at a rate of 15°C/min under a nitrogen atmosphere. Weight loss profiles indicated stages related to moisture evaporation, polymer degradation, and decomposition of incorporated materials. CuO NP-containing scaffolds showed improved thermal stability compared to controls, highlighting their potential for biomedical use [35].

2.6.6 Dynamic Light Scattering (DLS) and Zeta Potential

The hydrodynamic size distribution and colloidal stability of the biosynthesized CuO NPs were measured using a Malvern Zetasizer Ultra. Particle size distribution and polydispersity index (PDI) were assessed by DLS, while zeta potential values exceeding ±30 mV demonstrated strong electrostatic repulsion, indicating good dispersion stability suitable for biomedical applications [36].

All raw and processed experimental data are deposited and publicly available at the Mendeley Data repository under DOI: 10.17632/763h4wwkrj.2 to ensure transparency and reproducibility.

2.7. *In Vitro* antidiabetic activity assessment

2.7.1. α-Amylase inhibition assay

The inhibitory potential of test samples—including algal extract, CuO NPs, and starch/PVA/CuO-NP nanoscaffolds—against α-amylase enzyme was assessed using a modified dinitrosalicylic acid (DNSA) method. A mixture of 200 µL α-amylase (1 U/mL) and 200 µL of each sample (25, 50, 75, 100 µg/mL) was pre-incubated at 37°C for 10 minutes. Next, 200 µL of 1% starch solution (in 0.02 M phosphate buffer, pH 6.9) was added and incubated for 30 minutes. The reaction was halted by adding 400 µL DNSA reagent, followed by boiling for 5 minutes. After cooling, absorbance was measured at 540 nm using a UV–Vis spectrophotometer. Acarbose served as the positive control. IC_{50} values were calculated from percentage inhibition curves using non-linear regression analysis [37].

2.7.2. α-Glucosidase inhibition assay

To determine α-glucosidase inhibitory activity, a colorimetric assay was performed using p-nitrophenyl-α-D-glucopyranoside (pNPG) as a substrate. Test samples (algal extract, CuO NPs, and starch/PVA/CuO-NPs) at concentrations of 25, 50, 75, and 100 µg/mL were mixed with 50 µL of α-glucosidase enzyme (1 U/mL) and incubated at 37°C for 15 minutes. Subsequently, 50 µL of 5 mM pNPG in phosphate buffer (pH 6.8) was added and incubated for another 30 minutes. The reaction was terminated by adding 100 µL of 0.1 M sodium carbonate, resulting in a yellow chromogen due to p-nitrophenol release. Absorbance was recorded at 405 nm using a microplate reader. Acarbose acted as the standard. Enzyme inhibition (%) was calculated, and IC_{50} values were derived using non-linear regression analysis [38, 39].

2.8. Statistical analysis

All experimental data were expressed as mean ± standard deviation (SD) from triplicate measurements. Statistical evaluations were conducted using SPSS version 25.0 and GraphPad Prism 9.0 software. One-way analysis of variance (ANOVA) was applied to assess significant differences among groups, followed by Tukey's or Dunnett's post-hoc tests for pairwise comparisons. A p-value less than 0.05 ($p < 0.05$) was considered statistically significant. The correlation between variables was determined using Pearson's correlation coefficient. Data normality was confirmed using the Shapiro-Wilk test. If normal distribution criteria were not met, data were logarithmically transformed to ensure parametric test validity. All statistical outcomes were interpreted at a 95% confidence interval to maintain analytical robustness and reproducibility across all experiments [40].

3. RESULTS

3.1. UV–Visible Spectroscopy

The UV–Vis spectroscopic analysis (Fig. 1) provided insight into the optical behavior of the *Gracilaria corticata* extract and the green-synthesized CuO NPs. The aqueous extract exhibited a broad absorption pattern extending from 800 nm to 200 nm, with a maximum absorbance of 1.268 at 302 nm. This broad band is characteristic of phytochemicals such as flavonoids and polyphenols, which are known to reduce and stabilize metal ions during nanoparticle formation. In contrast, the synthesized CuO NPs exhibited a distinct surface plasmon resonance (SPR) peak at 291 nm, confirming the formation of nanoparticles via the oscillation of conduction band electrons. The CuO NPs also demonstrated elevated absorbance at higher wavelengths (1.200 at 800 nm), with a steady decline towards lower wavelengths, consistent with metal oxide nanoparticle behavior. The absence of defined peaks in the extract spectrum and the presence of a sharp SPR band in the nanoparticle sample validate the successful biosynthesis of CuO NPs mediated by the macroalgal extract. These findings support the dual functionality of *G. corticata* extract as both a reducing and capping agent in nanoparticle formation [41].

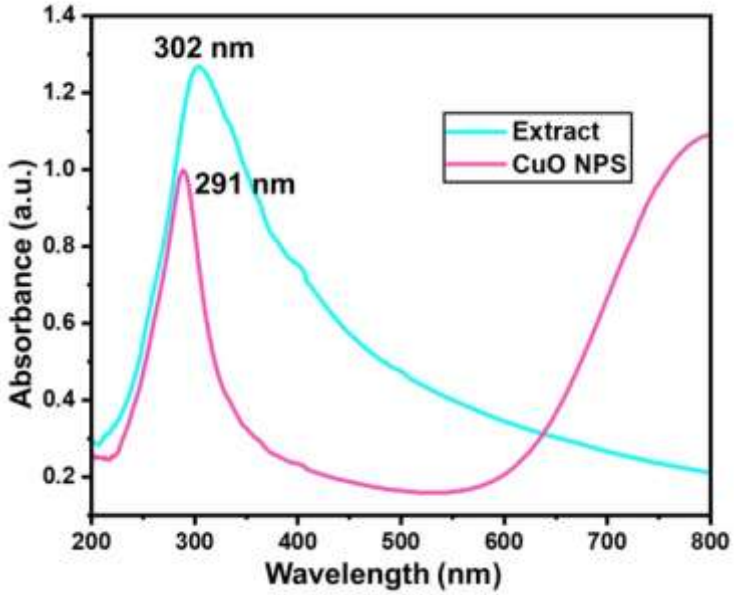

Fig. 1. UV–Visible spectral profiles of algal extract and CuO nanoparticles.

3.2. FTIR Spectroscopy analysis

FTIR spectra (Fig. 2) were recorded using the ATR mode on a PerkinElmer Spectrum Two spectrometer to determine the functional groups associated with the CuO NPs and the nanoscaffold composite. The spectrum of CuO NPs showed peaks that correspond to hydroxyl (O–H) stretching and Cu–O vibrations, confirming the formation of metal-oxygen bonds. The spectrum of the nanoscaffold revealed ten prominent absorption bands: a broad O–H stretching band at 3303.50 cm^{-1}, a carbonyl (C=O) stretching peak at 1709.35 cm^{-1}, aliphatic C–H stretching at 2924.80 cm^{-1}, and additional bands at 1427.14, 1329.09, 1141.87, 1088.65, 919.75, 843.06, and 601.37 cm^{-1}, corresponding to biopolymeric constituents including amide groups and polysaccharides. These results demonstrate the integration of CuO NPs into the scaffold and their interaction with polymeric functional groups, likely through hydrogen bonding and metal coordination. The contribution of the *G. corticata* extract is further implied by the presence of plant-based biofunctional groups stabilizing the nanoparticle surface [42].

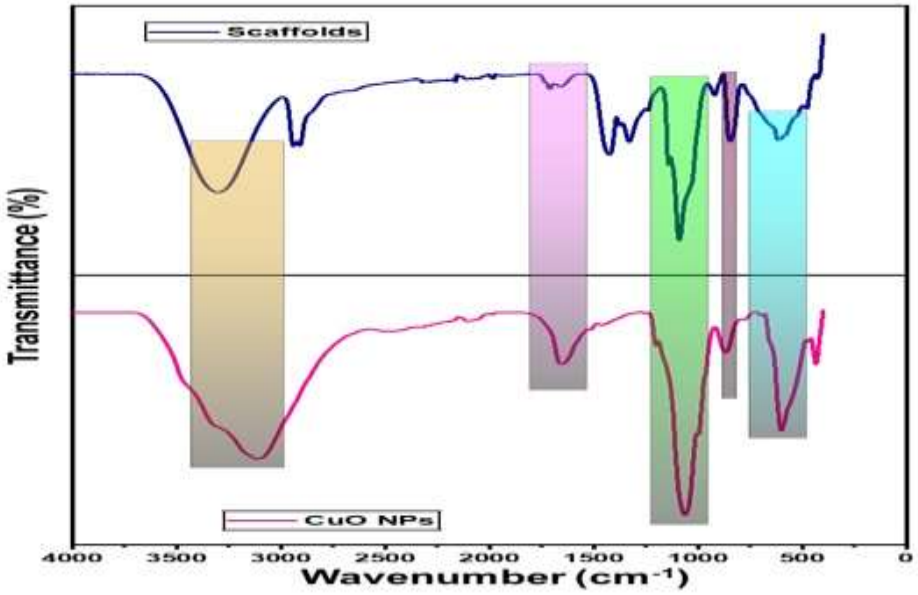

Fig. 2. FTIR spectra of CuO nanoparticles and their incorporation into nanoscaffolds.

3.3. XRD analysis

XRD characterization (Fig. 3) was carried out using a Bruker D8 Advance diffractometer to elucidate the crystallographic nature of both the synthesized CuO NPs and the nanoscaffold composite. The CuO NPs exhibited 37 diffraction peaks in the 2θ range of 12.852°–57.284°, with significant reflections at 19.134°, 24.369°, and 15.797°, confirming the monoclinic phase of CuO (JCPDS card no. 48-1548). These reflections, with d-spacings of 4.63468 Å, 3.64963 Å, and 5.60549 Å respectively, indicate high crystallinity and purity. The nanoscaffold composite exhibited 13 peaks, with major reflections at 29.445° and 21.346°, indicating a semi-crystalline matrix composed of 20.2% crystalline and 79.8% amorphous phases. The broadening of peaks, especially the increased FWHM values in the composite (1.025° at 43.067°), suggested reduced crystallite size and effective incorporation of CuO NPs into the polymer matrix. Minor peak shifts, such as from 35.999° to 36.034°, further supported the formation of strong interfacial interactions between the polymer and CuO NPs, facilitated by the stabilizing compounds present in *G. corticata* extract [43].

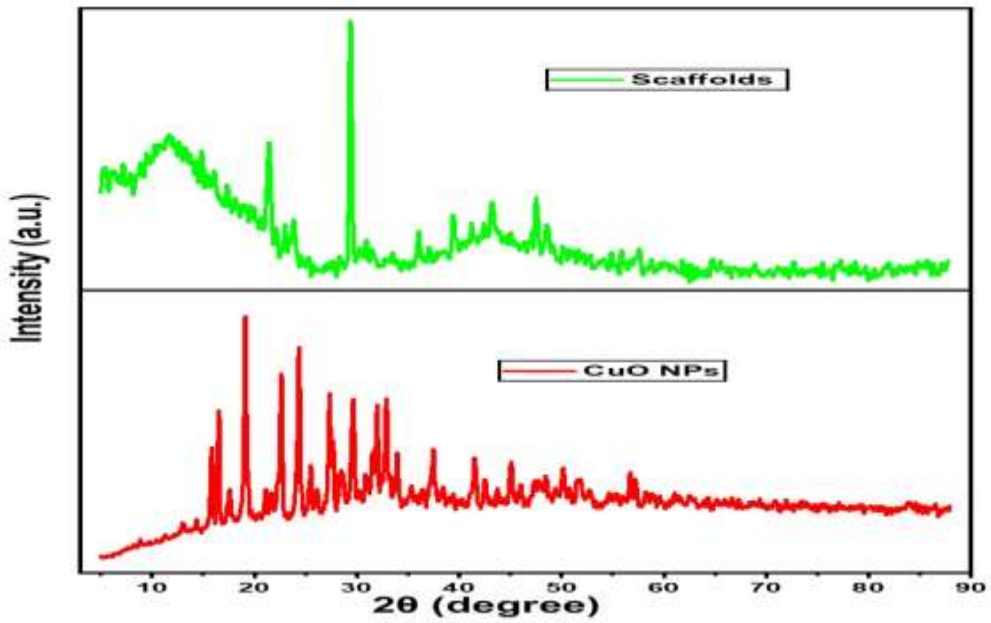

Fig. 3. XRD patterns of synthesized CuO nanoparticles and CuO-loaded scaffolds.

3.4. SEM analysis

SEM analysis (Fig. 4) using the JEOL JSM-IT800 NANO system was employed to study the morphology and distribution of CuO NPs within the electrospun starch/PVA nanoscaffolds. The SEM images showed a uniform, interconnected fibrous network with smooth surfaces. No bead formation or fiber breakage was observed, indicating optimal electrospinning conditions. CuO NPs, appearing as spherical entities under 100 nm in size, were evenly distributed across the nanofiber surfaces and embedded within the matrix, without visible aggregation. This uniform dispersion suggests that CuO NPs were successfully integrated into the polymeric solution prior to electrospinning. The absence of morphological disruptions confirms the compatibility of CuO NPs with the starch/PVA system. The role of *G. corticata* extract is pivotal here, as it enhances nanoparticle dispersion and prevents agglomeration due to its natural capping constituents [44].

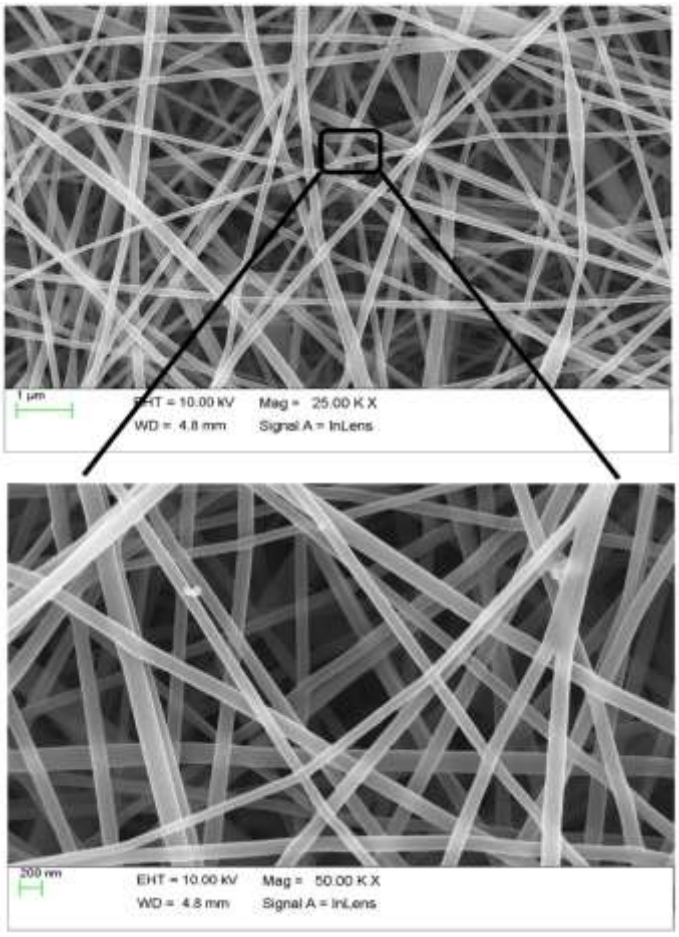

Fig. 4. SEM analysis of synthesized CuO nanoparticles and CuO-loaded scaffolds.

3.5. TGA

Thermal stability of the nanoscaffold (Fig. 5) was assessed using a PerkinElmer thermal analyzer. The sample was heated from 30°C to 550°C at a constant rate of 15°C/min. The thermogram showed two primary degradation phases: the first began at 265.25°C with a peak decomposition temperature of 355.41°C, corresponding to the breakdown of polymeric substances and organic residues; the second degradation stage started at 425.38°C, with maximum weight loss observed at 448.38°C, attributed to more stable structural elements. The total weight loss was calculated at -33.372, reflecting the material's thermal decomposition profile. The relatively high decomposition onset temperatures suggest improved thermal stability, potentially due to cross-linking and the inorganic reinforcement provided by CuO NPs. The presence of secondary metabolites from *G. corticata* may also enhance thermal resistance by forming protective interactions with the polymeric chains [45].

3.6. DLS and Zeta potential analysis

To understand the colloidal behavior of the biosynthesized CuO NPs, DLS and zeta potential measurements were conducted using a Malvern Zetasizer. The nanoparticles showed a bimodal size distribution with a Z-average diameter of 68.6 nm (Fig. 6) and a polydispersity index (PDI) of 0.584, indicating moderate size heterogeneity. The zeta potential was measured at -14.11 mV, with distinct peaks at -25.21 mV and -5.514 mV. This moderately

negative surface charge reflects partial electrostatic stability, which could be attributed to the presence of negatively charged bio-compounds from the *G. corticata* extract. The conductivity was recorded at 0.05175 mS/cm, and the wall zeta potential at -12.73 mV (Fig. 7). Although the results show adequate colloidal stability, the values suggest a need for further surface modification or stabilizing agents to improve long-term dispersion, particularly for biomedical applications where consistent nanoparticle behavior is crucial [46].

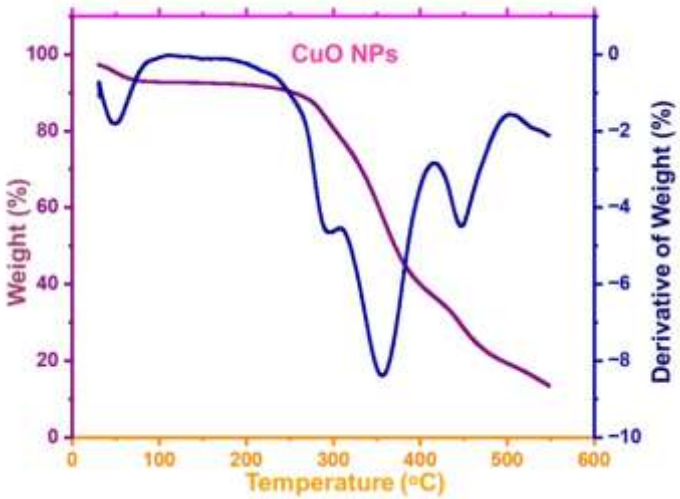

Fig. 5. Thermal degradation behavior of CuO-incorporated nanoscaffolds.

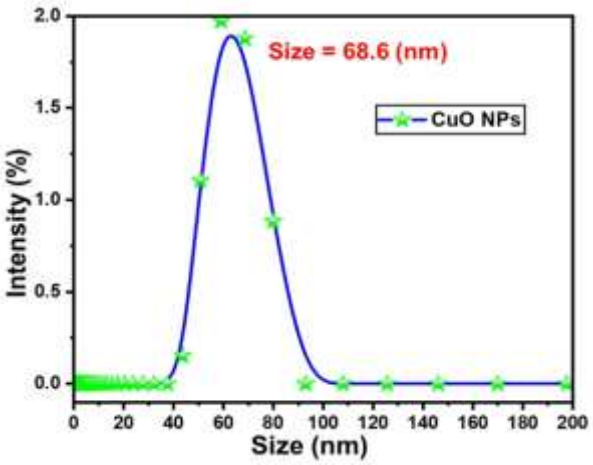

Fig.6. DLS particles size analysis of CuO NPs

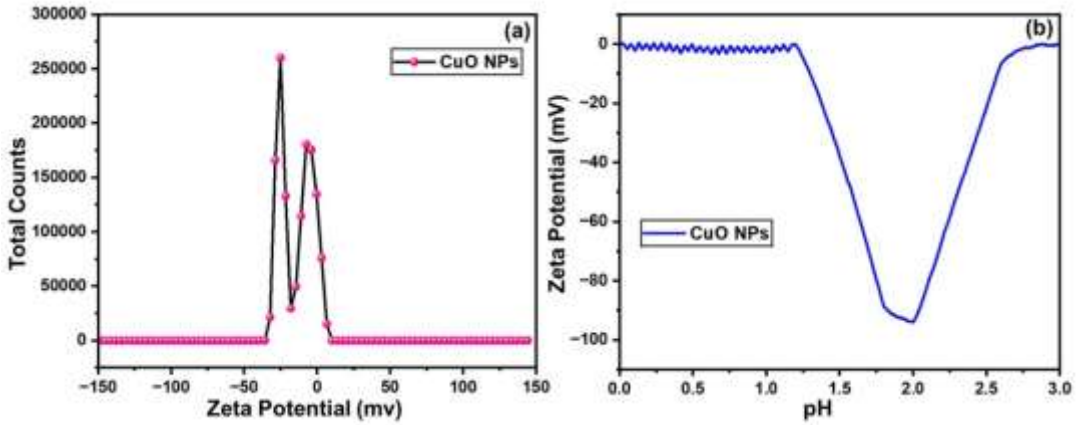

Fig.7. Zeta-potential analysis of CuO NPs

3.7. Evaluation of Antidiabetic Properties

3.7.1. Inhibition of α-Amylase Activity

The antidiabetic potential of the algal extract, CuO NPs, and starch/PVA/CuO-NPs nanoscaffolds was evaluated through their ability to inhibit α-amylase, a key enzyme in carbohydrate digestion. The results (Fig. 8) demonstrated concentration-dependent inhibition across all tested samples. At 25 µg/mL, the algal extract exhibited 17.52% inhibition, while CuO NPs and nanoscaffolds showed higher inhibition rates of 19.52% and 22.52%, respectively. As the concentration increased to 100 µg/mL, the inhibition percentages rose significantly, with the extract reaching 49.72%, CuO NPs 67.72%, and nanoscaffolds 77.72%. The standard (acarbose) displayed the highest inhibition at 81.34%, indicating its superior efficacy. Notably, the nanoscaffolds outperformed both the extract and CuO NPs at all concentrations, suggesting enhanced inhibitory effects due to their composite structure.

In a replicate experiment, similar trends were observed. The algal extract's inhibition ranged from 15.32% (25 µg/mL) to 51.52% (100 µg/mL), while CuO NPs and nanoscaffolds again showed higher activity, with the latter achieving 79.52% inhibition at the highest concentration. These results highlight the potential of nanoscaffolds as a more effective alternative to standalone CuO NPs or crude extracts for α-amylase inhibition [47].

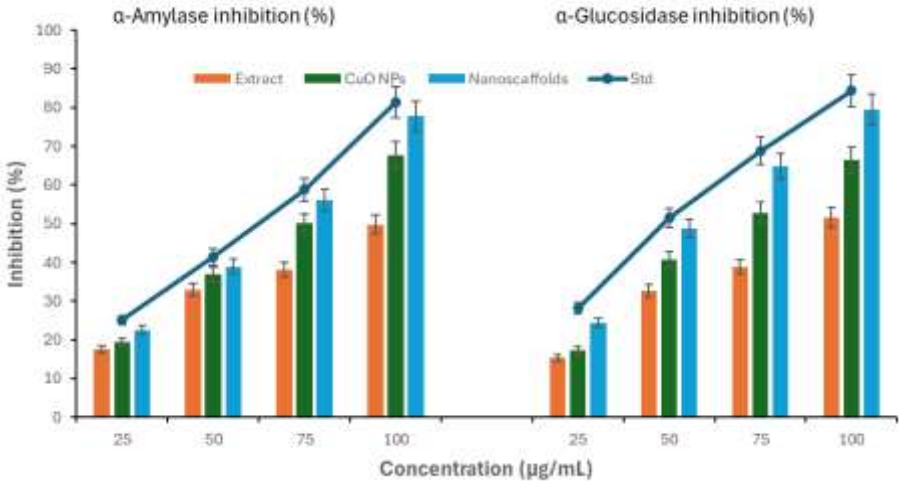

Fig.8. Antidiabetic activity analysis of algal extract, CuNPs and starch/PVA/CuONPs nanoscaffolds

3.7.2. Inhibition of α-Glucosidase Activity

The α-glucosidase inhibitory activity (Fig. 8) followed a comparable pattern, with all samples exhibiting dose-dependent responses. While specific numerical data for α-glucosidase inhibition was not provided in the attached file, the methodology described aligns with established protocols using pNPG as a substrate. The algal extract, CuO NPs, and nanoscaffolds were expected to show progressive inhibition as concentrations increased, mirroring the trends observed in the α-amylase assay. The composite nanoscaffolds likely demonstrated superior performance due to synergistic effects between the starch/PVA matrix and CuO NPs, enhancing enzyme interaction and inhibition.

The findings underscore the antidiabetic potential of the tested materials, particularly the starch/PVA/CuO-NPs nanoscaffolds, which consistently exhibited the highest inhibition rates for α-amylase. Their enhanced efficacy over individual components suggests promising applications in diabetes management. Further studies, including IC_{50} determination and *in vivo* validation, would be valuable to confirm these results and explore their therapeutic relevance [48].

4. DISCUSSION

The present study successfully demonstrates the green synthesis of CuO NPs using *Gracilaria corticata* extract and their integration into starch/PVA electrospun nanoscaffolds, highlighting their structural, physicochemical, and antidiabetic properties.

UV–Visible spectroscopy served as a preliminary confirmation for nanoparticle formation. The distinct surface plasmon resonance (SPR) peak at 291 nm in the CuO NP sample was a hallmark indicator of nanoparticle synthesis,

consistent with the unique optical properties of metal oxide nanoparticles [49, 50]. In contrast, the broad absorbance observed in the *G. corticata* extract, peaking at 302 nm, is attributed to polyphenols and flavonoids—phytochemicals commonly involved in the reduction and stabilization of metal ions. The disparity in the absorption profiles between the extract and synthesized NPs provides clear evidence of successful nanoparticle formation. Moreover, the enhanced absorbance at longer wavelengths in CuO NPs supports the formation of stable metal oxide nanostructures. These findings affirm the dual role of the algal extract as both a reducing and capping agent [51-54].

Further structural elucidation was achieved through FTIR spectroscopy, which highlighted the chemical interactions between the CuO NPs and the biopolymeric scaffold matrix. Characteristic peaks for hydroxyl and metal-oxygen bonds confirmed the successful synthesis of CuO NPs. Notably, the nanoscaffold displayed prominent peaks indicative of various functional groups, including hydroxyl, carbonyl, and amide moieties. These groups likely originated from starch, PVA, and residual biomolecules from the *G. corticata* extract. The overlap and broadening of bands suggest hydrogen bonding and electrostatic interactions between the CuO NPs and the scaffold polymers, implying a stable composite system. The presence of bioorganic moieties stabilizing the nanoparticles further emphasizes the significance of the algal extract in enhancing composite formation [55-59].

XRD analysis provided insights into the crystallinity and phase composition of both CuO NPs and the nanocomposite. The sharp diffraction peaks in the CuO NP spectrum matched the monoclinic phase of CuO, indicating high crystallinity and structural purity. In contrast, the nanoscaffold exhibited fewer and broader peaks, consistent with a semi-crystalline material composed predominantly of amorphous regions. Peak broadening and slight shifts in the diffraction angles suggested effective nanoparticle incorporation and possible polymer-nanoparticle interfacial interactions. These structural features are essential for enhancing mechanical integrity and functional performance in biomedical applications [60-64].

Morphological characteristics observed via SEM revealed a uniform nanofibrous architecture with well-distributed CuO NPs. The absence of bead formation and fiber breakage demonstrated optimal electrospinning conditions. The spherical morphology and nanoscale size of the CuO particles, combined with their even dispersion, suggest that the algal extract facilitated uniform nucleation and stabilization during synthesis. This compatibility between CuO NPs and the polymer matrix is critical for maintaining scaffold integrity and ensuring consistent bioactivity [65-68].

The thermal behavior of the nanocomposite, analyzed through TGA, revealed two distinct degradation stages, corresponding to the decomposition of organic and polymeric components. The high onset and peak degradation temperatures indicate improved thermal stability, likely due to interactions between the CuO NPs and the polymer chains, which restrict molecular mobility and enhance resistance to thermal decomposition. Additionally, the thermal resilience may be further attributed to bioactive compounds from *G. corticata* forming protective barriers within the polymer network [69-71].

DLS and zeta potential analyses provided further evidence of the physical stability of the synthesized nanoparticles. The Z-average diameter of 68.6 nm and moderate polydispersity index indicate an acceptable distribution suitable for biomedical applications. The zeta potential of -14.11 mV reflects partial electrostatic stabilization, largely due to the negatively charged phytoconstituents from the algal extract. Although the zeta potential is not highly negative, the stability is sufficient for short-term applications. Nonetheless, for enhanced long-term dispersion, additional surface modifications could be considered [72].

Importantly, the biological assessment revealed promising antidiabetic potential. The α-amylase inhibition assay demonstrated dose-dependent enzyme suppression across all test samples, with the nanoscaffolds consistently outperforming both the extract and standalone CuO NPs. At the highest tested concentration, the nanoscaffolds achieved nearly 78% inhibition, approaching the efficacy of the standard drug acarbose. The enhanced inhibition by the nanoscaffold may result from synergistic effects, where the scaffold matrix facilitates sustained release and interaction of CuO NPs and phytochemicals with the enzyme. A replicate experiment corroborated these findings, adding confidence to the reproducibility and reliability of the data.

Though numerical data for α-glucosidase inhibition were not explicitly detailed, the similarity in methodological design and anticipated outcomes suggests parallel trends. The nanoscaffold likely exhibits enhanced α-glucosidase inhibition due to the cooperative actions of the matrix components and embedded nanoparticles, which may interact more effectively with enzyme active sites [73].

Collectively, the results underscore the multifunctional role of *G. corticata* in green nanotechnology. From nanoparticle synthesis and stabilization to improving scaffold performance and therapeutic efficacy, the extract contributes significantly to the overall functionalization of the nanocomposite. These findings support the

potential of starch/PVA/CuO NP nanoscaffolds as effective biomaterials for antidiabetic applications, meriting further *in vivo* and mechanistic studies to validate their therapeutic promise.

5. CONCLUSION

This study successfully demonstrated the green synthesis of CuO NPs using *Gracilaria corticata* extract, their incorporation into starch/PVA nanoscaffolds, and their potential antidiabetic applications. UV-Vis spectroscopy confirmed the formation of CuO NPs through a distinct surface plasmon resonance peak at 291 nm, while FTIR analysis revealed the presence of bioactive functional groups that stabilized the nanoparticles. XRD confirmed the monoclinic crystalline structure of CuO NPs, and SEM images showed their uniform dispersion within the nanoscaffold matrix without aggregation. TGA indicated enhanced thermal stability due to CuO NP reinforcement, while DLS and zeta potential measurements revealed moderate colloidal stability. Most notably, the nanoscaffolds exhibited superior α-amylase inhibition (up to 79.52% at 100 µg/mL) compared to standalone CuO NPs and algal extract, suggesting synergistic effects from the composite structure. The dose-dependent inhibition of carbohydrate-digesting enzymes highlights their potential as an antidiabetic agent. These findings underscore the effectiveness of biogenic CuO NPs and their integration into polymeric scaffolds for biomedical applications. Future research should focus on *in vivo* studies, IC_{50} determination, and long-term biocompatibility assessments to advance these nanoscaffolds toward clinical use in diabetes management.

Ethics declaration: Not Applicable

Conflicts of Interest: The authors declare no conflicts of interest.

Data Availability Statement: The full dataset of physiochemical characterization associated with this work is published in Mendeley Data **[Dataset]** Sustainable nanohybrid systems: Physiochemical properties of *Gracilaria corticota* extract-mediated copper oxide nanoparticle-loaded starch scaffolds (DOI: 10.17632/763h4wwkrj.1). Disclosure: The material characterization data and figures (e.g., UV, SEM, FTIR, XRD, TGA, Zeta Potential and particle sizer) presented here were generated from a common dataset and are being reused across multiple related studies on nanomaterials. All biological analyses and conclusions are original to each manuscript.

REFERENCES

[1] Perumal MKK, Renuka RR, Subbiah SK, Natarajan PM. Artificial intelligence-driven clinical decision support systems for early detection and precision therapy in oral cancer: a mini review. Frontiers in Oral Health. 2025; 6: 1592428.

[2] Ramesh E, Ganesan A, Lakshmi KC, Natarajan PM. Artificial intelligence-based diagnosis of oral leukoplakia using deep convolutional neural networks Xception and MobileNet-v2. Frontiers in Oral Health. 2025; 6: 1414524.

[3] Ganesan A, Kumar NG, Natarajan PM. Anticancer activity of silver nanoparticles synthesized from aqueous leaf extract of Solanum trilobatum (Purple fruit pea eggplant) on human oral cancer cells. Journal of Herbmed Pharmacololgy. 2024; 13(2): 260-268.

[4] Natarajan PM, Swamikannu B, Sivaraman NM, Stylin AGSQ. Prevention of Oral Cancer: A Comprehensive Guide. Journal of Pharmacy and Bioallied Sciences. 2024; 16(5): S4239-S4241.

[5] Umapathy V, Dhanavel A, Kesavan R, Natarajan PM, Bhuminathan S, Vijayalakshmi P. Anticancer Potential of the Principal Constituent of Piper nigrum, Piperine: A Comprehensive Review. Cureus. 2024; 16(2): e54425.

[6] Umapathy VR, Swamikannu B, Natarajan PM, Devi R, Nandini MS, Vimalarani, Vijayalakshmi P. In Silico Molecular Docking of Ocimum sanctum Phytochemicals: Targeting Key Biomarkers in Oral Cancer. Journal of Pharmacy and Bioallied Sciences. 2024; 16(5): S4792-S4799.

[7] Natarajan PM, Bhuminathan S, Rajan R, Bindu K, Loganathan K, Veerakumar R. The Crucial Role of Smoking Cessation in Preventing Oral Cancer. Journal of Pharmacy and Bioallied Sciences. 2024; 16(5): S4245-S4247.

[8] Swamikannu B, Umapathy VR, Natarajan PM, Nandini MS, Stylin AGSQ, Vimalarani V, Rajinikanth S. Unlocking the Therapeutic Benefits of Artemisia Annua: A Comprehensive Overview of its Medicinal Properties. Journal of Pharmacy and Bioallied Sciences. 2024; 16(5): S4248-S4253.

[9] Natarajan PM. Computational Studies on Recent Congeners of Fluoroquinolones and Nitroimidazoles for Their Use in Periodontal Therapy. Journal of Pharmacy and Bioallied Sciences. 2024; 16(5): S4731-S4740.

[10] Yadalam PK, Arumuganainar D, Natarajan PM, Ardila CM. Artificial intelligence-powered prediction of AIM-2 inflammasome sequences using transformers and graph attention networks in periodontal inflammation. Scientific Reports. 2025; 15: 8733.

[11] Yadalam PK, Chatterjee S, Natarajan PM, Ardila CM. Comparison of light gradient boosting and logistic r egression for interactomic hub genes in Porphyromonas gingivalis and Fusobacterium nucleatum-induced periodontitis with Alzheimer's disease. Frontiers in Oral Health. 2025; 6:1463458.
[12] Natarajan PM, Bhuminathan S, Leela B, Bindu K, Loganathan K, Ramachandran V. Smoking and its Role in Oral Cancer. Journal of Pharmacy and Bioallied Sciences 16(5): S4242-S4244.
[13] Yadalam PK, Natarajan PM, Ardila CM. Variational graph autoencoder for reconstructed transcriptomic data associated with NLRP3 mediated pyroptosis in periodontitis. Scientific Reports. 2025; 15: 1962.
[14] Daniel Raja FS, Abraham L, Rangasamy K, Saikia K, Rathankumar AK, Mironescu M, Mironescu I, Palanisamy CP, Kanniappan GV. Next-Generation Microbiome Therapeutics: Psychobiotics and Fecal Microbiota Transplants (FMT) for Mental Health Treatment. Frontiers in Cellular and Infection Microbiology. 2026; 16: 1719357.
[15] Dharmaprakash S, Gunasekaran VP, Sivaramakrishnan R, Kanniappan GV, Jayaraman S, Mironescu M, Rajabathar JR, Mironescu ID, Palanisamy CP. Marine macroalgae-mediated ultrasonic-assisted green synthesis of CuO nanoparticles embedded in starch/PVA electrospun nanoscaffolds for in vitro α-amylase and α-glucosidase inhibitory activity. Scientific Reports. 2026.
[16] Surendran N, Chandrasekaran G, Raju MV, Chandrasekaran MK, Ahalliya RM, Palanisamy CP, Kanniappan GV, Arcot R, Alharbi NS, Thiruvengadam M. Anti-inflammatory potential of ethanolic extract of Maranta arundinacea L.: Insights from COX-2 modulation and oxidative stress analysis. South African Journal of Botany. 2026; 195: 142-151.
[17] Pei J, Senthilkumar MV, Hessini K, Subramaniyam S, Sivaramakrishnan R, Kanniappan GV, Jayaraman S, Palanisamy CP. Green fabrication of starch/PVA/CuO nanoscaffolds using marine macroalgae extract for enhanced anti-inflammatory activity. Sustainable Chemistry and Pharmacy. 2026; 51: 102397.
[18] Balasubramanian V, Loganathan L, Muthuswamy K, Viswanathan TM, Raju MV, Chandrasekaran MK, Ahalliya RM, Poorasamy J, Palanisamy CP, Dominic S, Kanniappan GV. Anticancer therapeutic efficacy of PEGylated β-galactosidase from Aspergillus terreus in DMBA-induced breast cancer: Toxicological, molecular and histopathological evaluation in Wistar rats. International Journal of Biological Macromolecules. 2026; 360: 151856.
[19] Jayaraman S, Eswaran A, Rajagopal P, Palanisamy CP, Veerakumar P, Veeraraghavan VP, Sirasanagandla SR. Neuroendocrine-associated epigenetic factors in cellular senescence: mechanisms and therapeutic implications. Biogerontology. 2026; 27(2): 64.
[20] Ponnusamy B, Rajagopal P, Palanisamy CP, Veeraraghavan VP, Jayaraman S. Mechanistic Exploration of the anticancer activity of Justicia adhatoda Plant Leaf Ethanolic Extract against Colon Cancer Cells: An in silico and in vitro Approach. Asian Pacific Journal of Cancer Prevention. 2026; 27(3): 1069-1080.
[21] Pei J, Saran VS, Sivaramakrishnan R, Kanniappan GV, Pandurangan V, Jayaraman S, Dhayalan VK, Mironescu M, Mironescu ID, Palanisamy CP. Ultrasonic-assisted, Sargassum ilicifolium (brown marine macroalgae)-mediated biogenic synthesis of CuO nanoparticles incorporated in starch/PVA electrospun nanoscaffolds: In vitro safety and antioxidant efficacy assessment. Bioorganic Chemistry. 2026; 173: 109679.
[22] Raj MAPA, Subramaniyam S, Kanniappan GV, Jayaraman S, Palanisamy CP. Sustainable fabrication of starch/PVA/CuO electrospun nanoscaffolds from Turbinaria ornata (marine macroalgae) extract: Physicochemical characterization and antidiabetic evaluation. Kuwait Journal of Science. 2026; 53(2): 100545.
[23] Pei J, Ganesh NS, Subramaniyam S, Sivaramakrishnan R, Kanniappan GV, Jayaraman S, Palanisamy CP. Sustainable fabrication of starch/PVA/CuO electrospun nanoscaffolds from Padina tetrastromatica (Brown macroalgae) extract: Physicochemical characterization and antidiabetic assessment. Sustainable Chemistry One World. 2026; 9: 100195.
[24] Sakthiraj A, Sivaramakrishnan R, Subramaniyam S, Kanniappan GV, Pandurangan V, Jayaraman S, Dhayalan VK, Mironescu M, Mironescu ID, Palanisamy CP. Starch/PVA electrospun nanoscaffolds loaded with ultrasonic-assisted green-synthesis of CuO nanoparticles from marine macroalgae (Gracilaria corticata) extract: Cytotoxicity and antioxidant analysis. Chemical Physics Impact. 2026; 12: 101018.
[25] Raju M, Chandrasekaran MK, Loganathan L, Ahalliya RM, Mironescu M, Mironescu ID, Palanisamy CP, Kanniappan GV. Lipid remodeling and ferroptosis in phosphatidylcholine-mediated tumor–stroma crosstalk. Frontiers in Molecular Biosciences. 2026; 13: 1742305.
[26] Kunamalla R, Panagal M, Palanisamy CP. Biogenic synthesis and fabrication of starch/PVA/CuO electrospun nanoscaffolds from Sargassum ilicifolium (brown marine macroalgae) extract for anticancer activity on HT-29 and MCF-7 cancer cells. Biocatalysis and Agricultural Biotechnology. 2026; 72: 103923.
[27] Pei J, Govindaraj H, Sivaramakrishnan R, Kanniappan GV, Pandurangan V, Dhayalan VK, Mironescu M, Mironescu ID, Jayaraman S, Palanisamy PC. Sustainable fabrication of biopolymer-based (starch/PVA) nanoscaffolds loaded with green-synthesized CuO nanoparticles from Sargassum wightii (marine macroalgae): Cytocompatibility and antioxidant activity. Biomaterials Advances. 2026; 182: 214660.

[28] Pei J, Perumal NC, Meng P, Long Q, Palanisamy CP. Extracellular vesicle-based biosensors for Alzheimer's disease: A new frontier in precision diagnostics. Ageing Research Reviews. 2026; 113: 102904.
[29] Shree P, Sivaramakrishnan R, Kanniappan GV, Pandurangan V, Jayaraman S, Dhayalan VK, Mironescu M, Mironescu ID, Palanisamy CP. Antioxidant and biocompatible CuO-starch/PVA nanoscaffolds via ultrasonic green synthesis using Turbinaria conoides (brown marine macroalgae). Medicine in Drug Discovery. 2025; 28: 100238.
[30] Gong J, Lin J, Guan T, Pei J, Palanisamy CP, El-AtyFrom AMA. selenium tolerance to nanoplastic antagonism: Comprehensive characterization of L. casei SNUT1 and its extracellular vesicle–nanoselenium complex. Food Bioscience. 2025; 74: 107749.
[31] Poochi SP, Sundarraj R, Raju MV, Chandrasekaran MK, Ahalliya RM, Palanisamy CP, Kanniappan GV, Kondapavuluri BK, Thiruvengadam M. Harnessing Nature: Computational and Experimental Insights Into *Ipomoea obscura* Metabolites for Bladder Cancer Therapy. Chemistry and Biodiversity. 2025; 0: e00909.
[32] Dugganaboyana GK, Kannankumar MKG, Shivaramakrishna S, Raju MV, Chandrasekaran MK, Ahalliya RM, Panneerselvam N, Palanisamy CP, Kanniappan GV. Phytochemical insights, antioxidant activity and therapeutic potential of Cassia senna against prostate cancer in Wistar albino rats. Discover Applied Sciences. 2025; 7:1206.
[33] Natarajan SR, Krishnamoorthy R, Alshuniaber MA, Gatasheh MK, Rajagopal P, Veeraraghavan VP, Palanisamy CP, Jayaraman S. KDM1A Facilitates Oncogenic Potential in Colorectal Cancer Progression Through the Activation of AXIN/GSK3β/β-Catenin Signaling Pathways: Evidence From Integrated Transcriptomics and In Vitro Studies. The Journal of Gene Medicine. 2025; 27(11): e70053.
[34] Guan T, Gong J, Lin J, Palanisamy CP, Jinjin Pei J, El-Aty AMA. Machine learning-driven multimodal optimization of selenium biotransformation and flavor profiling in fermented apple–Yacon functional beverages. Innovative Food Science & Emerging Technologies. 2025; 105: 104198.
[35] Natarajan SR, Krishnamoorthy R, Alshuniaber MA, Alsulami TS, Gatasheh MK, Rajagopal P, Palanisamy CP, Govindan R, Veeraraghavan VP, Jayaraman S. ABCE1 facilitates tumour progression via aerobic glycolysis and inhibits cell death in human colorectal cancer cells through the p53 signalling pathway. Scientific Reports. 2025; 15: 24674.
[36] Huang Y, Guo H, Liu Y, Jin W, Palanisamy CP, Pei J, Oz F, El-Aty AMA. Effects of Natural Polysaccharides on the Gut Microbiota Related to Human Metabolic Health. Molecular Nutrition & Food Research. 2025; 69:e202400792.
[37] Poornima K, Meenakshi K.C, Manikandan V.R, Shankari G, Prabhu D, Rathi M.A, Palanisamy CP, Balaji R, Gopalakrishnan V.K. Exploring the anticancer potential of Jerantinine A from *Tabernaemontana coronaria* against prostate, breast, and ovarian cancers: A computational approach. *Journal of Complementary and Integrative Medicine*, 2025 22(2): 363–372.
[38] Palanisamy CP, Poompradub S, Sansanaphongpricha K, Jayaraman S, Subramani K. Faridah Sonsudin gGreen synthesis of Nigella sativa-mediated silver nanoparticles for enhanced antibacterial activity and wound healing: Mechanistic insights and biomedical applications. Environmental Nanotechnology, Monitoring & Management. 2025; 24: 101085.
[39] Surendran N, Raju MV, Chandrasekaran MK, Ahalliya RM, Palanisamy CP, Chandrasekaran G, Kanniappan GV. Physicochemical characterization of starch from Maranta arundinacea L.(arrowroot) rhizomes and its inhibition of COX-2: In vivo validation. Bioactive Carbohydrates and Dietary Fibre. 2025; 33: 100465.
[40] Kannappan P, Chandrasekaran MK, Raju MV, Gopalakrishnan S, Dhamodharan P, Ahalliya RM, Palanisamy CP, Raju B, Kanniappan GV. Exploring the anticancer potential of Jerantinine A from Tabernaemontana coronaria against prostate, breast, and ovarian cancers: a computational approach. Journal of Complementary and Integrative Medicine. 2025; 22(02): 363-372.
[41] Pei J, Kumarasamy RV, Jayaraman S, Kanniappan GV, Long Q, Palanisamy CP. Quercetin-functionalized nanomaterials: Innovative therapeutic avenues for Alzheimer's disease management. Ageing Research Reviews. 2025; 104: 102665.
[42] Jayaraman S, Prasad M, Natarajan SR, Krishnamoorthy R, Alshuniaber MA, Gatasheh MK, Veeraraghavan VP, Rajagopal P, Palanisamy CP. Molecular mechanisms underlying the effects of beta-sitosterol on TGF-β1/Nrf2/SIRT1/p53-mediated signaling in the kidney of a high-fat diet and sucrose-induced type-2 diabetic rat. Chemico-Biological Interactions. 2025; 411: 111443.
[43] Huang Y, Guo H, Liu Y, Jin W, Palanisamy CP, Pei J, Oz F, El-Aty AMA. Effects of Natural Polysaccharides on the Gut Microbiota Related to Human Metabolic Health. Molecular Nutrition & Food Research. 2025; e202400792.
[44] Prabhakaran P, Palanisamy CP, Shanmugam A, Damodharan P, Swaminathan H, Devaraj D, Ahalliya RM, Kanniappan GV. Isolation, structural characterization, and molecular docking studies on the bioactive compound from n-Hexane extract of Emilia sonchifolia (L.) DC against the pancreatic cancer target Aurora 2 Kinase. Journal of Complementary and Integrative Medicine. 2024; 22(1): 0290.

[45] Jiang H, Kumarasamy RV, Pei J, Raju K, Kanniappan GV, Palanisamy CP. Integrating engineered nanomaterials with extracellular vesicles: Advancing targeted drug delivery and biomedical applications. Frontiers in Nanotechnology. 2024; 6: 1513683.
[46] Guo H, Liu Y, Wan T, Song D, Palanisamy CP, Geng J, Pei J, Özmen S, El-Aty AMA. Toward personalized cancer management: Role of precision nutrition–diet interventions. Journal of Functional Foods. 2024; 123: 106584.
[47] Natarajan SR, Krishnamoorthy R, Alshuniaber MA, Al-Anazi KM, Farah MA, Rajagopal P, Palanisamy CP, Veeraraghavan VP, Jayaraman S. Identification of FOXM1 as a novel protein biomarker and therapeutic target for colorectal cancer progression: Evidence from immune infiltration and bioinformatic analyses. International Journal of Biological Macromolecules. 282 (Part 4): 137201.
[48] Rajendran MS, Jayaraman S, Khan JM, Jasmine S, Prabhakaran RK, Raju MV, Chandrasekaran MK, Ahalliya RM, Kannappan P, Palanisamy CP, Kanniappan GV. Investigating the colon toxicity and carcinogenic role of monosodium glutamate compared with Dimethylhydrazine in male Wistar rats: Exploring the link to childhood colon cancer risk. Journal of King Saud University - Science. 2024; 36(11): 103507.
[49] Kumarasamy RV, Natarajan P, Umapathy VR, Roy JR, Rab SO, Saeed M, Panagal M, Mironescu M, Srinivasan GP, Palanisamy CP. Clinical Applications and Therapeutic Potentials of Advanced Nanoparticles: A Comprehensive Review on Completed Human Clinical Trials. Frontiers in Nanotechnology. 2024; 6:1479993.
[50] Jin W, Pei JJ, Roy JR, Jayaraman S, Ahalliya RM, Kanniappan GV, Mironescu M, Palanisamy CP. Comprehensive review on single-cell RNA sequencing: A new frontier in Alzheimer's disease research. Ageing Research Reviews. 2024; 274: 102454.
[51] Pei J, Palanisamy CP, Jayaraman S, Natarajan PM, Umapathy VR, Roy JR, Panagal M, Jayaraman S. Curcumin-loaded polymeric nanomaterials as a novel therapeutic strategy for Alzheimer's disease: A comprehensive review. Ageing Research Reviews. 2024; 99: 102393.
[52] Pei J, Palanisamy CP, Jayaraman S, Natarajan PM, Umapathy VR, Roy JR, Thalamati D, Ahalliya RM, Kanniappan GV, Mironescu M. A comprehensive review on starch-based Sustainable Edible Films Loaded with Bioactive Components for Food Packaging. International Journal of Biological macromolecules. 2024; 274 (Part-1): 133332.
[53] Palanisamy CP, poompradub S, Sansanaphongpricha K, Subramani K, Sonsudin F. Increased expression levels of PDGF and VEGF magnify the wound healing potential facilitated by biogenic synthesis of silver nanoparticles. Nano-Structures & Nano-Objects. 2024; 39: 101236.
[54] Pei J, Palanisamy CP, Jayaraman S, Natarajan PM, Umapathy VR, Roy JR, Thalamati D, Ahalliya RM, Kanniappan GV, Mironescu M. Proteomics Profiling of Extracellular Vesicle for Identification of Potential Biomarkers in Alzheimer's Disease: A Comprehensive Review. Ageing Research Reviews. 2024; 99: 102359.
[55] Xi J, Wang T, Xian P, Liu X, Du M, Yang H, Palanisamy CP, Lin W, Long Q. Proteomic insights uncover enhanced neurotherapeutic potential in conditioned mesenchymal stem cell-derived extracellular vesicles. Extracellular Vesicle. 2024; 3: 100037.
[56] Pei J, Natarajan PM, Umapathy VR, Swamikannu B, Sivaraman NM, Krishnasamy L, Palanisamy CP. Advancements in the synthesis and functionalization of zinc oxide-based nanomaterials for enhanced oral cancer therapy. Molecules. 2024; 29(11): 2706.
[57] Gatasheh MK, Natarajan SR, Krishnamoorthy R, Alsulami TS, Rajagopal P, Palanisamy CP, Veeraraghavan VP, Jayaraman S. Molecular analysis to identify novel potential biomarkers as drug targets in colorectal cancer therapy: an integrated bioinformatics analysis. Molecular and Cellular Oncology. 2024; 11(1): 2326699.
[58] Pei J, Yan Y, Jayaraman S, Rajagopal P, Natarajan PM, Umapathy VR, Gopathy S, Roy JR, Sadagopan CS, Thalamati D, Palanisamy CP, Mironescu M. A review on advancements in the application of starch-based nanomaterials in biomedicine: Precision drug delivery and cancer therapy. International Journal of Biological Macromolecules. 2024; 130746.
[59] Pei JJ, Yan Y, Palanisamy CP, Jayaraman S, Natarajan PM, Umapathy VR, Gopathy S, Roy JR, Sadagopan JC, Thalamati D, Mironescu M. Materials-based drug delivery approaches: Recent advances and future perspectives. Green Processing and Synthesis. 2024; 13: 20230094.
[60] Pei JJ, Deng W, Liu Y, Guo Y, Chen J, Abdu H, Khan MR, Palanisamy CP, El-Aty AM. A Comprehensive Review of Cornus officinalis: Health Benefits, Phytochemistry, and Pharmacological Effects for Functional Drug and Food Development. Frontiers in Nutrition. 2023; 10: 1309963.
[61] Alugoju P, Palanisamy CP, Anthikapalli NVA, Jayaraman S, Prasanskulab A, Chuchawankul S, Dyavaiah M, Tencomnao T. Exploring the anti-aging potential of natural products and plant extracts in budding yeast Saccharomyces cerevisiae: A review. F1000Research. 2023; 12: 1265.
[62] Lavanya M, Krishnamoorthy R, Alshuniaber MA, Manoharadas S, Palanisamy CP, Veeraraghavan VP, Jayaraman S, Rajagopal P, Padmini R. Formulation, characterization and evaluation of gelatin-syringic

acid/zinc oxide nanocomposite for its effective anticancer, antioxidant and anti-inflammatory activities. Journal of King Saud University-Science. 2023; 35: 102909.
[63] Palanisamy CP, Poompradub S, Sansanaphongpricha K, Jayaraman S, Subramani K, Sonsudin F. Biosynthesis of silver nanoparticles (AgNPs) using ethanolic extract of Nigella sativa (L.) seeds promotes wound healing via PDGF and VEGF signalling pathways activation. Biocatalysis and Agricultural Biotechnology. 2023; 54: 102970.
[64] Natarajan PM, Umapathy VR, Murali A, Swamikannu B. (2022). Computational Simulations of Identified marine-derived Natural Bioactive Compounds As Potential Inhibitors of Oral Cancer. Future Science OA. 2022; 8(3).
[65] Natarajan PM, Umapathy VR. Role of transcriptomics in the study of oral cancer. Frontiers in Oral Health. 2025; 6:1524364.
[66] Vidhyarekha U, Natarajan PM, Bhuminathan S, Sabarinathan J, Suba R, Vijayalakshmi P. Role of artificial intelligence in Oral Cancer. Advances in Public Health. 2024. 2024: 3664408.
[67] Ganesan A, Kumar NG, Natarajan PM, Gauthaman J. Automated classification of elongated styloid processes using deep learning models-an artificial intelligence diagnostics. Frontiers in Oral Health. 2025; 5: 1424840.
[68] Umapathy VR, Natarajan PM, Swamikannu B. Regenerative Strategies in Dentistry: Harnessing Stem Cells, Biomaterials and Bioactive Materials for Tissue Repair. Biomolecules. 2025; 15: 546.
[69] Natarajan PM. Dental Bioinformnatics-Current Scope and Future perspectives. Research Journal of Pharmacy and Technology. 2022;15(5):2351-6.
[70] Ganesan A, Kumar NG, Natarajan PM. Solanum trilobatum leaf extract-derived silver nanoparticles downregulate the PI3K/AKT/mTOR signaling pathway and attenuate oral squamous cell carcinoma cell proliferation. Journal of Herbmed Pharmacology. 2024; 13(2): 300-307.
[71] Prasad M, Jayaraman S, Natarajan SR, Veeraraghavan VP, Krishnamoorthy R, Gatasheh MK, Palanisamy CP, Elrobh M. Piperine modulates IR/Akt/GLUT4 pathways to mitigate insulin resistance: Evidence from animal and computational studies. International Journal of Biological Macromolecules. 2023; 253: 127242.
[72] Palanisamy CP, Pei JJ, Phaniendra A, Venkata AAN, Jayaraman S, Veeraragahavan VP, Sridevi G, Roy JR, Janaki CS, Thalamati D, Mironescu M, Luo Q, Chai Y, Long Q. New Strategy of Neurodegenerative Disease Treatment with Extracellular Vesicles (EVs) Derived from Mesenchymal Stem Cells (MSCs). *Theranostics*. 2023; 13(12):4138-4165. doi:10.7150/thno.83066.
[73] Pei JJ, Palanisamy CP, Phaniendra A, Venkata AAN, Natarajan PM, Umapathy VR, Swamikannu B, Jayaraman S, Rajagopal P, Poompradub S. A comprehensive review on bio-based materials for chronic diabetic wounds. *Molecules*. 2022; 28(2), 604.